PLASMA PROFILE PREDICTION IN NSTX DISCHARGES USING THE UPDATED MULTI-MODE ANOMALOUS TRANSPORT MODULE

T. RAFIQ, C. WILSON, C. CLAUSER, E. SCHUSTER, J. WEILAND
Lehigh University
Bethlehem, PA, USA
Email: rafiq@lehigh.edu

J. ANDERSON
Chalmers University of Technology
Gothenburg, Sweden

S. KAYE, A. PANKIN, B. LEBlANC, R. BELL
Princeton Plasma Physics Laboratory,
Princeton, NJ, USA

Abstract

The objective of this study is twofold: firstly, to demonstrate the consistency between the anomalous transport results produced by updated Multi-Mode Model (MMM) version 9.1 and those obtained through gyrokinetic simulations; and secondly, to showcase MMM's ability to predict electron and ion temperature profiles in low aspect ratio, high beta NSTX discharges. MMM encompasses a range of transport mechanisms driven by electron and ion temperature gradients, trapped electrons, kinetic ballooning, peeling, microtearing, and drift resistive inertial ballooning modes. These modes within MMM are being verified through corresponding gyrokinetic results. The modes that potentially contribute to ion thermal transport are stable in MMM, aligning with both experimental data and findings from linear CGYRO simulations. The isotope effects on these modes are also studied and found to be stabilizing, consistent with the experimental trend. The electron thermal power across the flux surface is computed within MMM and compared to experimental measurements and nonlinear CGYRO simulation results. Specifically, the electron temperature gradient modes (ETGM) within MMM account for 2.0 MW of thermal power, consistent with experimental findings. It is noteworthy that the ETGM model requires approximately 5.0 ms of computation time on a standard desktop, while nonlinear CGYRO simulations necessitate 8.0 hours on 8 K cores. MMM proves to be highly computationally efficient, a crucial attribute for various applications, including real-time control, tokamak scenario optimization, and uncertainty quantification of experimental data.

1. INTRODUCTION

Predicting time-dependent electron and ion temperature profiles in the National Spherical Torus Experiment (NSTX) presents a challenge due to its low aspect ratio and high beta discharges, unlike conventional fusion devices with larger aspect ratios and lower beta discharges. Previously, an earlier version of the Multi-Mode Model (MMM) [1] was used in the integrated modeling code TRANSP [2] to successfully predict plasma profiles in conventional devices such as JET, DIII-D, EAST, and KSTAR [3]. The updated version, MMM 9.1, is now incorporated into TRANSP to demonstrate the consistency of MMM results with gyrokinetic simulations and its capability to predict electron and ion temperature profiles in NSTX discharges.

In the realm of gyrokinetic simulations, it's common practice to simulate only a few tens of microseconds of plasma time, which requires tens to hundreds of hours of computer simulation time before turbulence stabilizes into a quasi-steady state. Simulating processes on the timescale of a tokamak discharge, which can span tens to hundreds of seconds, necessitates the inclusion of physics-based fluid transport modules to accurately describe turbulence-driven anomalous transport.

The physics-based Multi-Mode Model (MMM) is a multi-species, multi-fluid, multi-mode anomalous transport model that calculates electron and ion thermal transport, electron particle transport, impurity transport, and toroidal and poloidal momentum transport in tokamak discharges. The MMM comprises four components: (i) the Weiland model for transport driven by ion temperature gradient (ITG), trapped electrons (TE), kinetic ballooning (KB), peeling, and high mode number MHD modes [4]; (ii) a new electromagnetic electron temperature gradient mode (ETGM) model for electron thermal transport [5]; (iii) an updated microtearing mode (MTM) model for transport driven by electron temperature gradients in both the collisionless and collisionality regimes [6]; and (iv) an updated model for the drift resistive inertial ballooning mode (DRIBM) for transport driven by gradients,

electron inertial effects, and inductive effects [7]. Numerous upgrades have been implemented to enhance the precision, consistency, speed, and physical basis of these MMM components. These improvements are crucial not only for the NSTX/NSTX-U but also for the development of reactor concepts based on spherical tokamaks.

The structure of this paper is outlined as follows: Section 2 presents the NSTX parameters pertaining to discharges with both high and low collisionality. Section 3 presents an analysis of the real frequency, growth rate, fluxes, and diffusivities of MMM when subjected to flow shear on and off conditions. The discussion also encompasses the impact of isotopes on unstable modes. Section 4 presents the results obtained using the MMM and compares them to the results generated by CGYRO [8]. Section 5 presents the predicted temporal profiles of NSTX discharges, specifically focusing on low and high collisionality discharges. Section 6 provides a conclusion of the results obtained from the MMM analysis, as well as a comparison of these results with those obtained from gyrokinetic simulations and experimental observations.

2. NSTX LOW AND HIGH COLLISIONALITY DISCHARGES

The NSTX high collisionality discharge (120968) and the low collisionality discharge (120982) are considered for the calculation of modes present in MMM. As can be seen in Fig.1, the input profiles, such as temperature, density, safety factor, and elongation, differ between both discharges, resulting in varying gradients. The effective electron beta, flow shear, and collision frequency are plotted in Fig.2, highlighting differences in the profiles. These profile variations will impact the stability of the modes, as well as thermal, particle, and momentum fluxes and diffusivities.
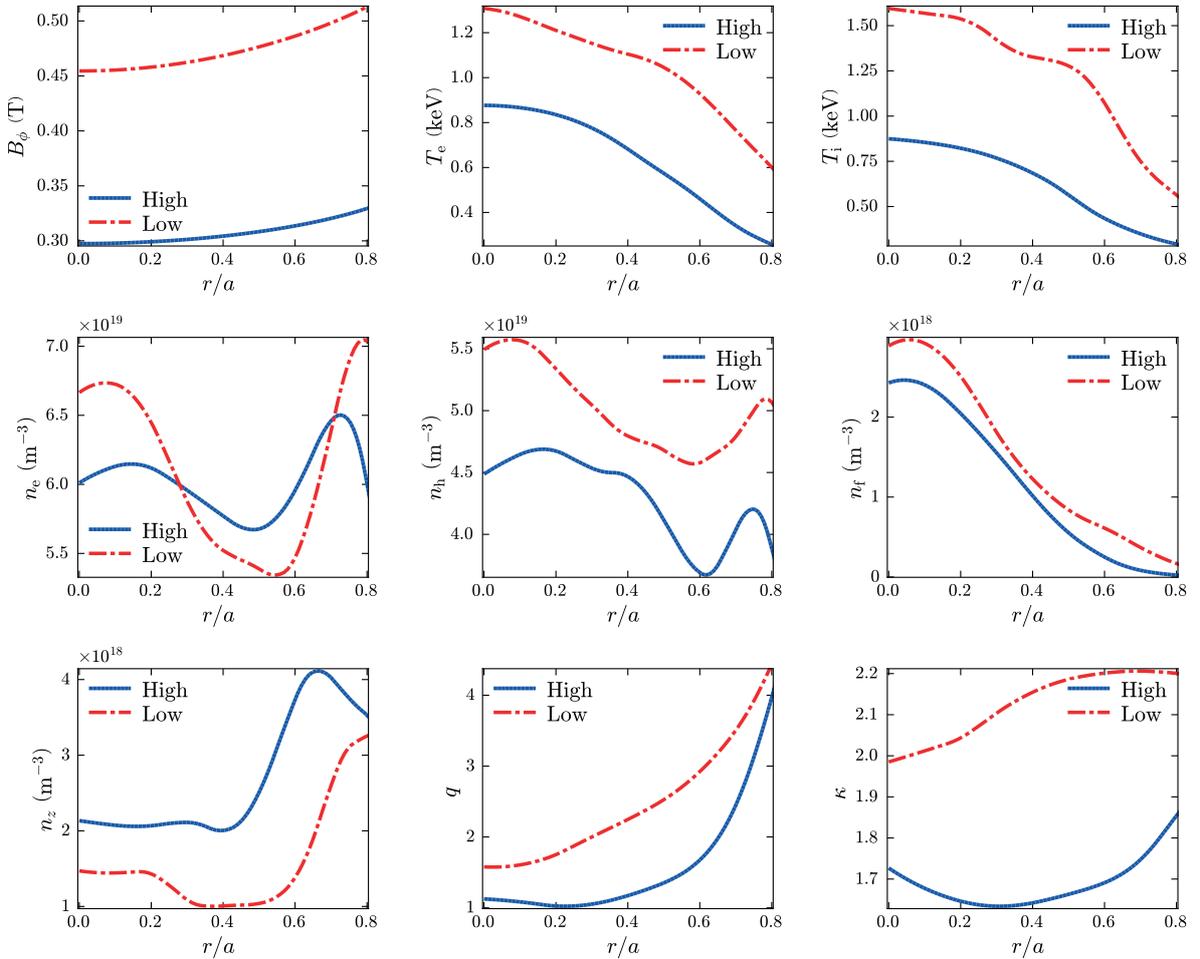

FIG. 1. Parameters for high collisionality discharge 120968 at t = 0.56 s and low collisionality discharge 120982 at t = 0.62 s, including toroidal magnetic field (B_ϕ), electron temperature (T_e), ion temperature (T_i), electron density (n_e), hydrogen density (n_h), fast ion density (n_f), impurity density (n_z), safety factor (q), and elongation (κ).

3. NUMERICAL RESULTS

The modes present in low and high collisionality discharges are shown below, both with and without the $\mathbf{E} \times \mathbf{B}$ flow shear effect, in order to determine the types of modes that are present, stabilized by flow shear, or have survived. The effects of isotopes on the growth rate of modes are also determined.
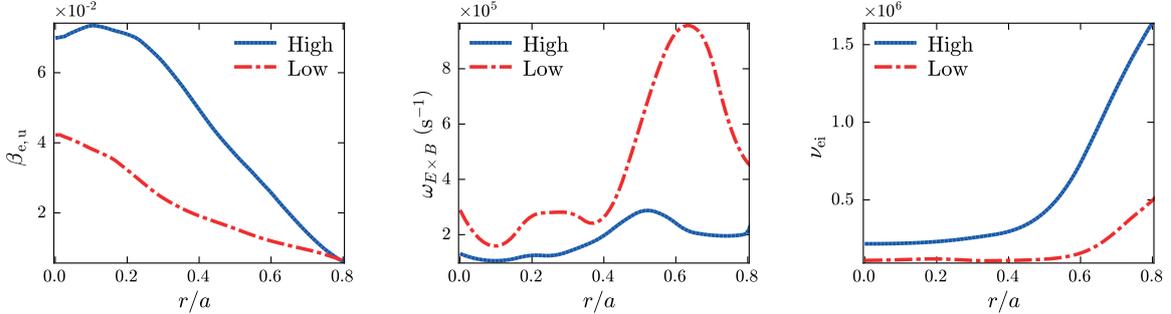

FIG. 2. The effective electron beta ($\beta_{e,u}$), $\mathbf{E} \times \mathbf{B}$ flow shear ($\omega_{E \times B}$), and electron-ion collision frequency (ν_{ei}) are shown for high and low collisionality discharges.

3.1. Results for low and high collisionality without the $\mathbf{E} \times \mathbf{B}$ flow shear effect

The growth rate and frequency of ITG/TEM ($\gamma_{i,w20}, \omega_{i,w20}$), ETGM ($\gamma_{etgm}, \omega_{etgm}$), MTM ($\gamma_{mtm}, \omega_{mtm}$), and DRIBM ($\gamma_{dbm}, \omega_{dbm}$) in the absence of flow shear are presented in Fig. 3 for high and low collisionality discharges. Note that $k_\theta \rho_s$ is not fixed at each surface; instead, a $k_\theta \rho_s$ scan is performed to determine the most unstable mode. Here, k_θ represents the poloidal wave vector, and ρ_s denotes the ion Larmor radius.

ITG/TEM instability is observed in both discharges, with these modes typically manifesting in the ion direction. Additionally, these modes show a strong correlation with variations in the ion temperature gradient within the plasma. It's noteworthy that these ITG/TEM modes have the potential to significantly influence ion thermal transport. However, in NSTX discharges, the primary mechanism governing ion thermal transport is neoclassical. This implies that neoclassical mechanisms, rather than ITG/TEM modes, primarily dictate ion thermal energy transport within the plasma in NSTX discharges. An intriguing aspect to consider is the potential impact of flow shear on the stability of these ITG/TEM modes, which will be explored in the next subsection.

The instability associated with ETG modes is electron-directional and linked to the electron temperature gradient within the plasma. ETG growth rates are larger in high collisionality discharge due to the significant electron temperature gradient compared to low collisionality discharge. ETG modes exhibit significantly higher growth rates than flow shear, although flow shear can mitigate their adverse effects on plasma confinement. Nevertheless, these modes persist even in the presence of flow shear and contribute to electron thermal transport. ETG modes are identified as the most unstable among all instabilities in flow shear-off conditions and are likely to play a pivotal role in electron thermal transport in both low and high collisionality NSTX discharges.

Microtearing modes, which rotate in the electron direction, are driven by gradients in electron temperature and density in the presence of collisionality, rendering them unstable. While in certain radial locations, the growth rate of MTM is higher in high collisionality cases, overall, the diffusivity attributed to MTM is expected to be greater in low collisionality cases throughout all radial positions. This phenomenon is due to the significantly elevated electron temperature in low collisionality cases, leading to a higher thermal velocity that amplifies transport effects. In the case of low collisionality discharges, MTM ion direction modes with a substantial growth rate are also observed in the region ($0.6 \leq r/a \leq 0.8$) with a negative electron density gradient (see g_{ne} in 5). MTMs display resilience in gyrokinetic simulations, even in the presence of flow shear [8]. Therefore, the influence of flow shear will be disregarded, allowing these modes to maintain their original growth rate and contribute to electron thermal transport.

DRIBMs exhibit a complex instability resulting from density and temperature gradients, electrical resistivity, plasma inertia, and pressure gradients. In low collisionality discharges, these modes are stable, while in high collisionality discharges, they become unstable toward the edge of the plasma. They rotate in the electron's direction. However, the growth rate of the unstable mode in high collisionality discharges is relatively smaller than the flow shear. Consequently, it's expected that these modes will not significantly contribute to thermal and particle transport in flow shear-on conditions.

CGYRO simulations have provided valuable insights into the stability of plasma modes in NSTX discharges across a wide range of collisionality scenarios. Notably, these simulations have shown that TEM, MTM, ETGM,

and KBM modes exhibit instability in both high and low collisionality discharges [8]. Of particular significance is the observation that, in both gyrokinetic and MMM simulations, the ETG mode emerges as the most unstable [9]. This mode's pronounced instability emphasizes its crucial role in driving electron thermal transport within the plasma, highlighting the importance of a comprehensive understanding and control strategies to enhance plasma confinement and fusion device performance.
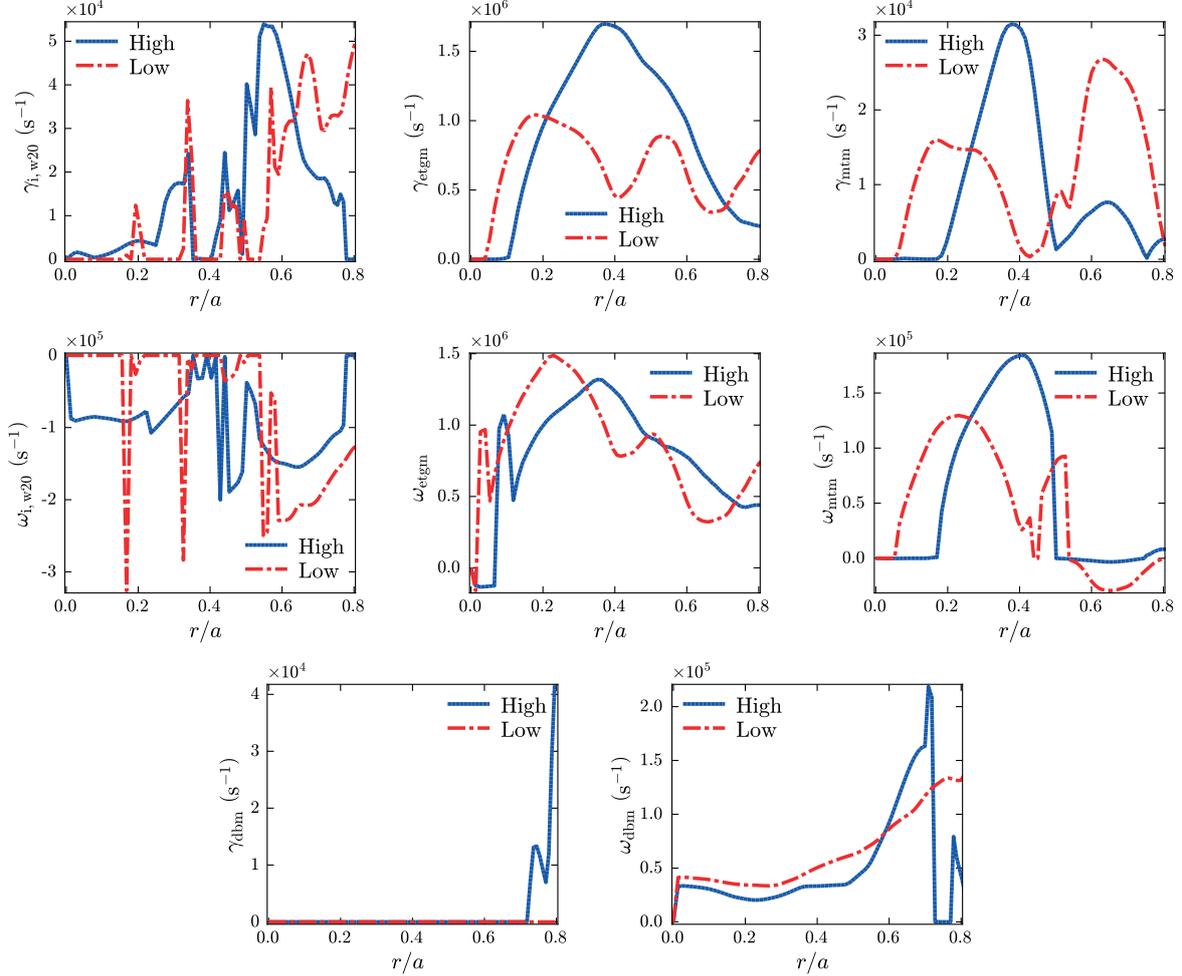

FIG. 3. The growth rate and frequency of various instabilities, namely ITG/TEM ($\gamma_{\mathrm{i,w20}}$, $\omega_{\mathrm{i,w20}}$), ETGM (γ_{etgm}, ω_{etgm}), MTM (γ_{mtm}, ω_{mtm}), and DRIBM (γ_{dbm}, ω_{dbm}), are shown in high and low collisionality NSTX discharges in the absence of flow shear.

Figure 4 displays the total electron thermal flux (Γ_{e}) and ion thermal flux (Γ_{i}), electron particle flux (Γ_{n}), toroidal momentum flux (Γ_{ϕ}), poloidal momentum flux (Γ_{θ}), and impurity flux (Γ_{z}). In Figure 5, we present the normalized electron temperature gradient (g_{Te}), normalized ion temperature gradient (g_{Ti}), magnetic shear (s), normalized electron density gradient (g_{ne}), and the normalized impurity density (g_{nz}) for both high and low collisionality NSTX discharges. Our observations reveal that in high collisionality discharges, there is a substantial electron thermal flux, primarily driven by a significant normalized electron temperature gradient and a high electron temperature. Conversely, in low collisionality scenarios, ion thermal flux dominates, primarily due to the pronounced normalized ion temperature gradient and low magnetic shear (s). It's worth noting that the DRIBM instability in the edge region disrupts this trend, leading to distinct transport behavior. Furthermore, our analysis identifies a strong correlation between particle flux and g_{ne}. Toroidal momentum flux is notably associated with the g_{Ti}, while poloidal momentum flux exhibits prominence in regions characterized by substantial pressure gradients. Notably, impurity particle flux exhibits a close relationship with the g_{nz}, with evident impurity pinch effects manifesting in regions marked by negative values of g_{nz}. This investigation unveils the intricate relationships between various gradient parameters and transport phenomena within fusion devices, shedding light on the underlying physics that govern these complex interactions. These findings contribute to our fundamental understanding of plasma behavior and hold promise for optimizing fusion device performance and mitigating
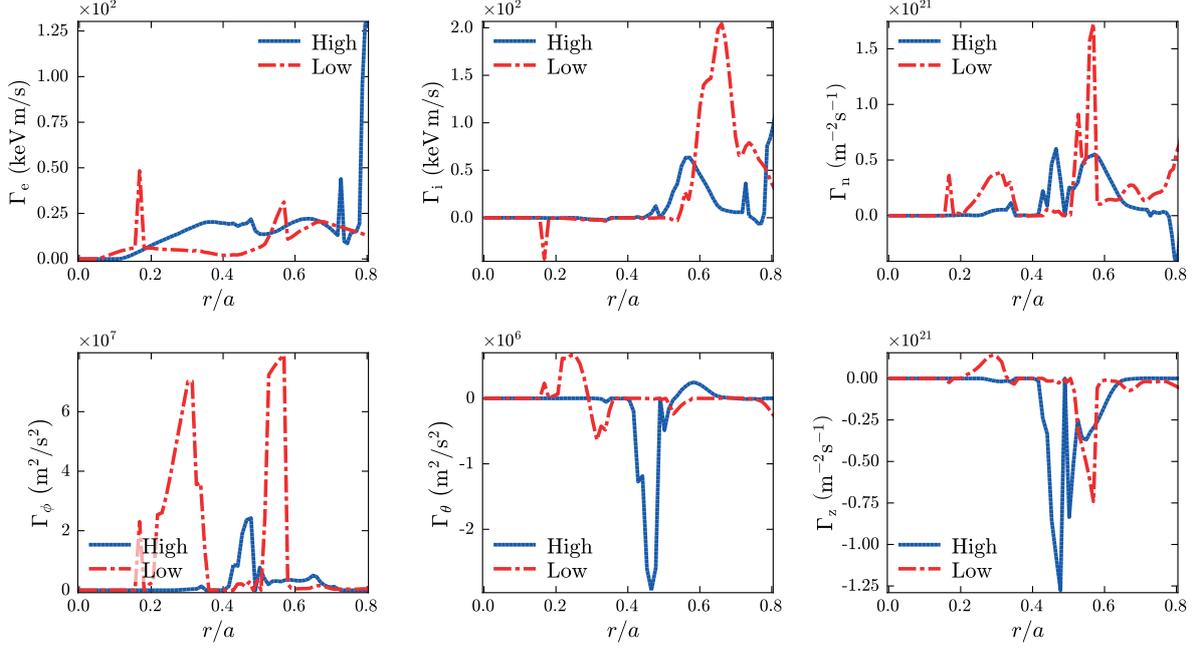
FIG. 4. Total electron thermal flux (Γ_e) and ion thermal flux (Γ_i), particle flux (Γ_n), toroidal momentum flux (Γ_ϕ), poloidal momentum flux (Γ_θ), and impurity flux (Γ_z), under flow shear-off conditions, in high and low collisionality NSTX discharges.
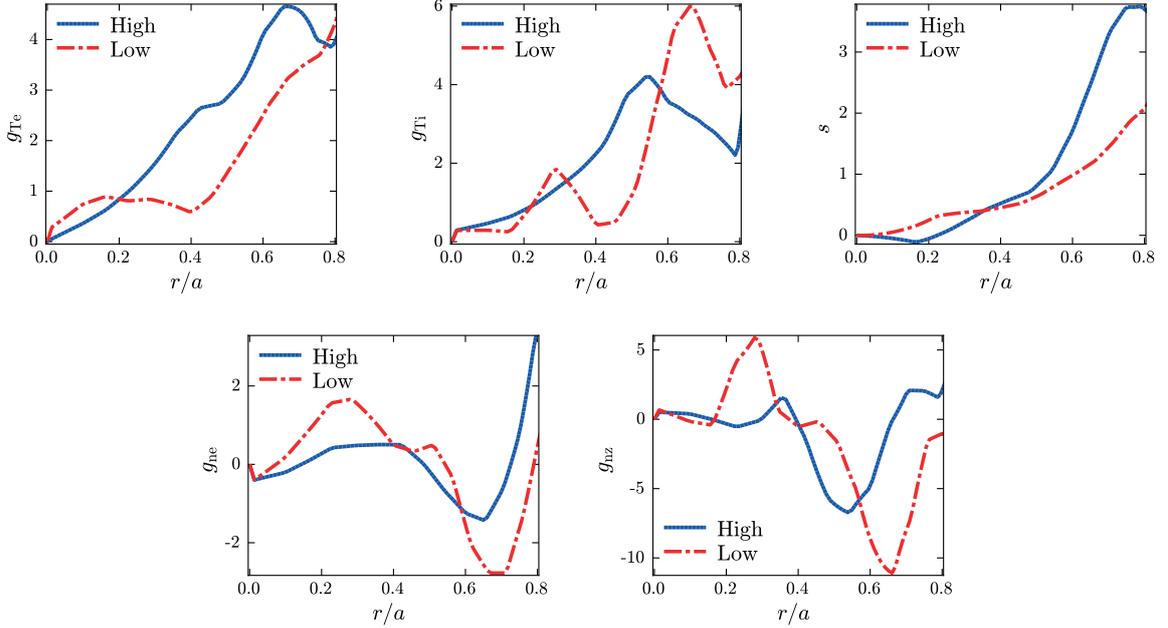

FIG. 5. Normalized electron temperature gradient (g_Te), normalized ion temperature gradient (g_Ti), magnetic shear (s), normalized electron density gradient (g_ne), and the normalized impurity density (g_nz) are plotted in high and low collisionality NSTX discharges.

undesirable transport effects.

3.2. Results for low and high collisionality with the E × B flow shear effect

The presence of **E** × **B** flow shear ($\omega_{E\times B}$) plays a crucial role in stabilizing or mitigating instabilities. In our numerical results, we take its effects into account. Instabilities like ITG/TEM/DRIBM/KBM, which contribute to ion thermal, particle, and momentum transport, are found to be stabilized by $\omega_{E\times B}$. As a result, we anticipate that the confinement region in NSTX discharges under consideration will not exhibit anomalous ion thermal, particle,

5

or momentum transport. Instead, the observed transports will follow neoclassical behavior. It's worth noting that we do not consider momentum transport caused by the ion-scale microtearing mode. The finding of neoclassical ion thermal transport aligns with both CGYRO simulations and experimental results.

In Figure 6, we present the growth rates (γ_{etgm}, γ_{mtm}) of the ETGM and MTM modes, their corresponding electron thermal diffusivities ($\chi_{\text{e,etgm}}$, $\chi_{\text{e,mtm}}$), and total electron thermal diffusivity (χ_{e}) in the presence of flow shear ($\omega_{E \times B}$). The ETGM mode demonstrates resilience, indicating anomalous thermal electron transport in NSTX discharges, consistent with both CGYRO simulations and experimental findings. In contrast, CGYRO results show that MTM (γ_{mtm}) is unaffected by flow shear, so flow shear is not activated for MTMs. ETGM (γ_{etgm}) is found to be less influenced by flow shear, except for $\hat{\rho} > 0.4$ in low collisionality cases where flow shear is substantial. The substantial growth rate of ETGM in high collisionality scenarios is primarily attributed to low flow shear and a significant electron temperature gradient. These factors also contribute to higher total electron thermal diffusivity in high collisionality discharges, as it is the sum of ETGM thermal diffusivity and MTM thermal diffusivity.
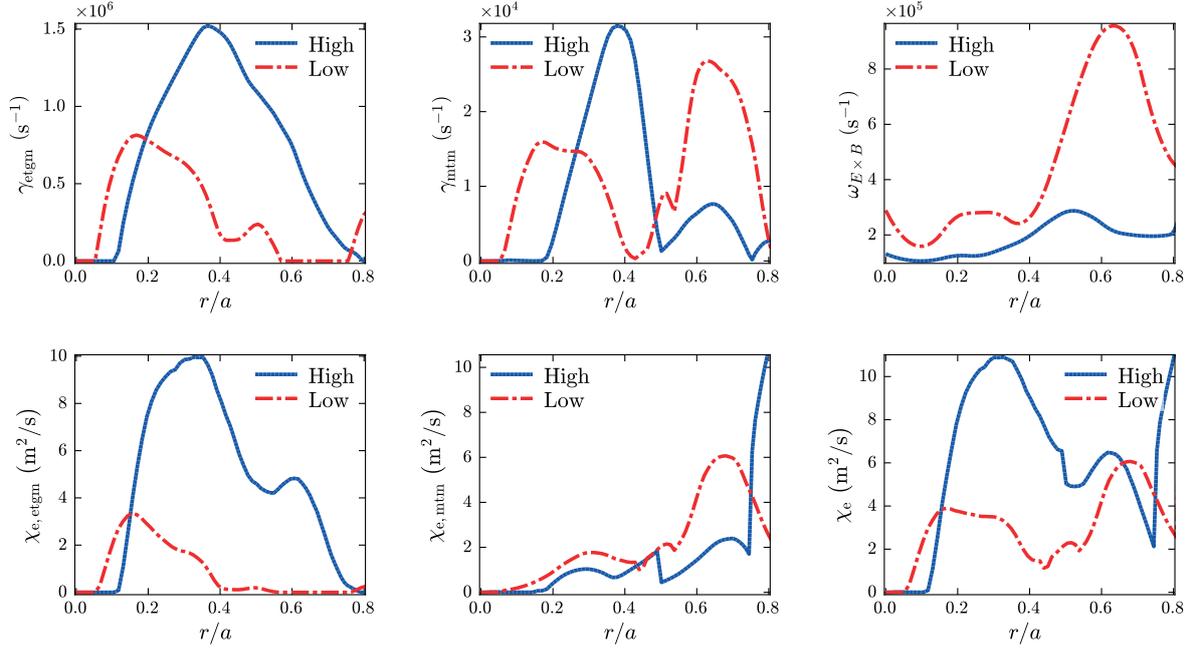

FIG. 6. ETGM growth rate (γ_{etgm}), MTM growth rate (γ_{mtm}), and $\mathbf{E} \times \mathbf{B}$ flow shear ($\omega_{E \times B}$), ETGM electron thermal diffusivity ($\chi_{\text{e,etgm}}$), MTM electron thermal diffusivity ($\chi_{\text{e,mtm}}$), and total electron thermal diffusivity (χ_{e}) are plotted in high and low collisionality NSTX discharges.

3.3. Effects of Isotopes

In our study, we explore the effects of isotopes (H, D, T) on the modes present in MMM for low and high collisionality discharges. Specifically, we examine the ITG/TEM growth rate ($\gamma_{\text{i,W20}}$), ETGM growth rate (γ_{etgm}), and MTM growth rate (γ_{mtm}), as displayed in Fig. 7 for hydrogen plasma (Figs in the first row) and tritium plasma (Figs in the second row) in both high and low collisionality discharges.

Our findings reveal that these isotope effects have a stabilizing impact on ITG/TEM/MTM and DRIBM (not shown here) modes, while they are relatively insignificant for ETGM. This observation can be attributed to tritium's higher mass, which reduces the thermal velocity of tritium ions. Consequently, they are less susceptible to rapid motion caused by temperature-driven random particle motion, thereby reducing their contribution to turbulence and transport. Furthermore, the inclusion of ion viscosity in MMM plays a crucial role in replicating the experimental trend, where transport is observed to decrease with higher ion mass.

4. COMPARISON OF ETGM TO ITS CORRESPONDING CGYRO MODES

The components of MMM undergo verification by comparing them to corresponding gyrokinetic results. Previously, the MTM model was verified against GYRO simulations, demonstrating close agreement between the MTM model in MMM and gyrokinetic results [10]. Here, we verify the newly developed electromagnetic ETGM model using CGYRO simulations, as illustrated in Fig. 8. Our findings show that the ETG-MMM model accurately reproduces the real frequency of ETG modes. Additionally, the magnitude of the most unstable mode in the $k_\theta \rho_s$
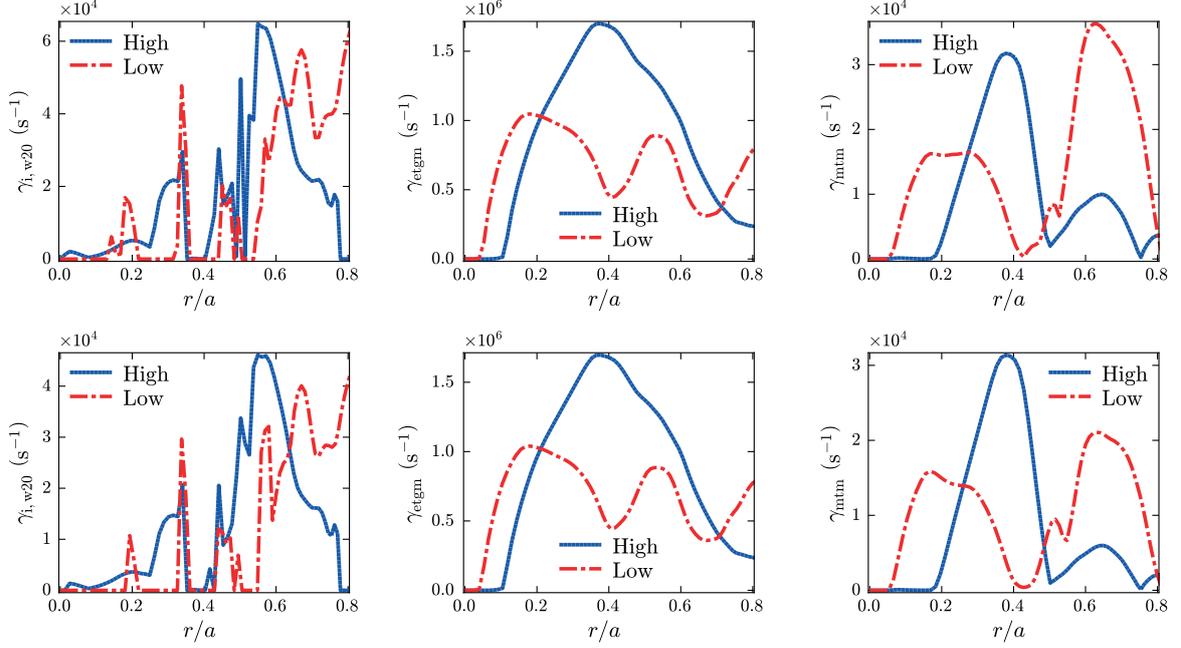
FIG. 7. ITG/TEM growth rate ($\gamma_{i,W20}$), ETGM growth rate(γ_{etgm}), and MTM growth rate (γ_{mtm}) are displayed for hydrogen plasma (first row) and tritium plasma (second row) for high and low collisionality discharges.

spectrum closely matches CGYRO results. Notably, the ETG-MMM mode stabilizes early in the $k_\theta \rho_s$ spectrum. This difference can be due to the way FLR effects are included in the ETG-MMM model, where the norm of $< k_\perp >$, based on a well-localized eigenfunction, is used. We further assess the total electron power across the flux surface using the ETG-MMM model and compare it to experimental measurements and nonlinear CGYRO simulation results. The ETG-MMM model yields 2.0 MW of thermal power, aligning with experimental data. In contrast, the CGYRO code yields 3.5 MW of thermal power in the nonlinear simulation. It's worth noting that the ETG-MMM model exhibits computational efficiency, requiring only approximately 5.0 ms of computation time on a standard desktop. In contrast, nonlinear CGYRO simulations demand 8.0 hours on 8 K cores.
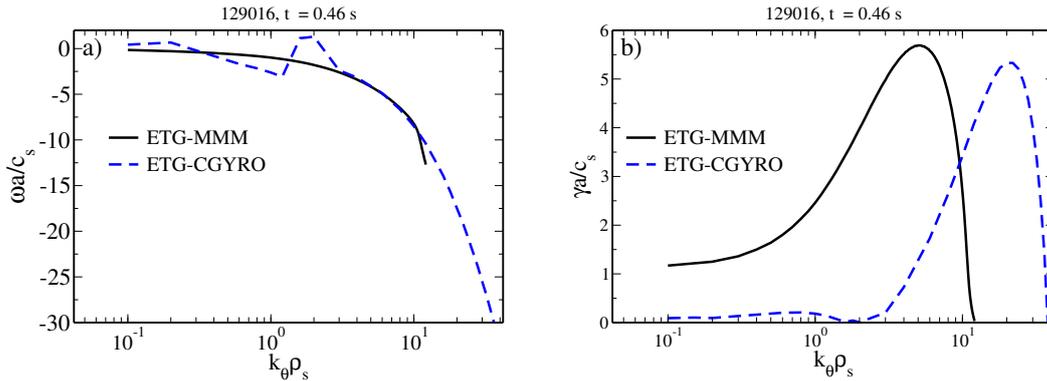

FIG. 8. ETG-MMM and ETG-CGYRO normalized frequency ($\omega a/c_s$) and growth rate ($\gamma a/c_s$) for a low collisionality discharge.

5. COMPARISON OF PREDICTED ELECTRON AND ION TEMPERATURES WITH EXPERIMENTAL DATA

The updated MMM model version 9.1 has been implemented in the integrated modeling code TRANSP [2]. This implementation allows for the prediction of electron and ion temperature profiles in NSTX discharges with varying collisionality, including both L-mode and H-mode scenarios. These predictions are then compared to the corresponding experimental profiles. Notably, the MMM model demonstrates excellent agreement between predicted profiles and experimental data, for high and low collisionality discharges, as shown in Fig. 9. Also shown are the ion and electron thermal diffusivities. MMM's versatility extends to the prediction of profiles for

temperature, electron density, current density, and rotation in both existing experiments and future thermonuclear fusion devices. Its exceptional computational efficiency is a critical asset, enabling various applications, including real-time control, tokamak scenario optimization, and uncertainty quantification of experimental data.
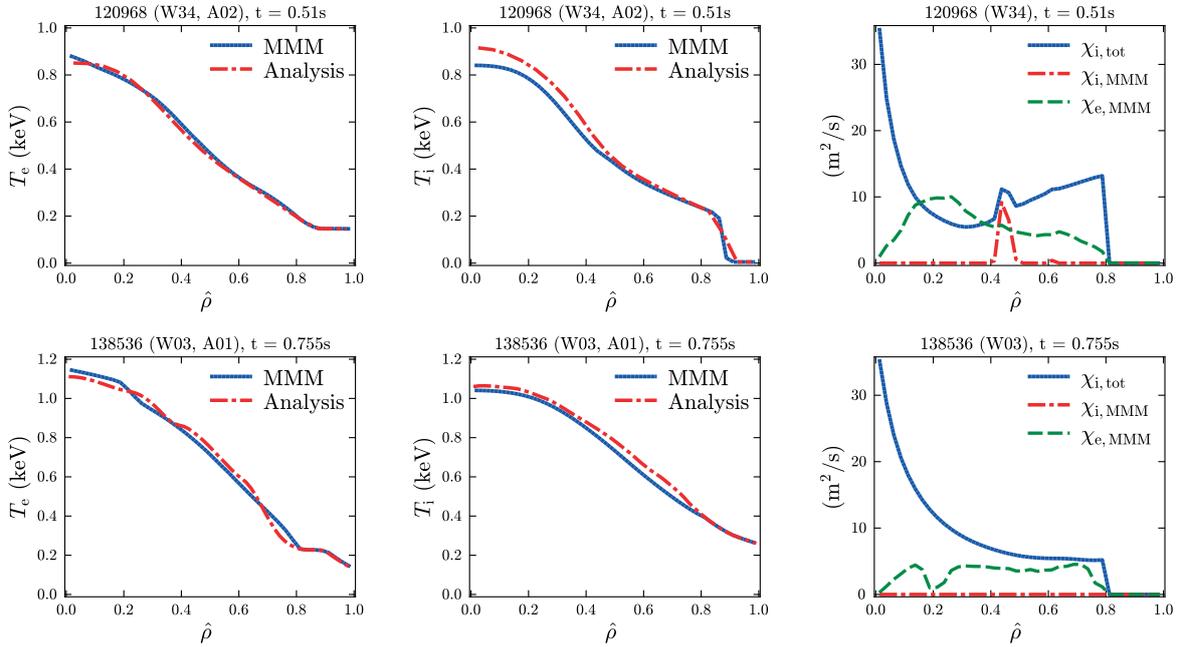

FIG. 9. Predicted (MMM) and analytical electron and ion temperature profiles, total ion thermal diffusivity ($\chi_{i,tot} = \chi_{neo} + \chi_{i,MMM}$), ion and electron thermal MMM diffusivities ($\chi_{i,MMM}, \chi_{e,MMM}$) for the high collisionality discharge 120968 at t = 0.51 s and for the low collisionality discharge 138536 at t = 0.75 s.

ACKNOWLEDGEMENTS

CONCLUSIONS

The study aims to demonstrate the consistency between MMM results and gyrokinetic simulations and to establish MMM's capability to predict electron and ion temperature profiles in low aspect ratio, high beta NSTX discharges. The stabilizing effect of isotopes in MMM simulations is also demonstrated. MMM simulations exhibit strong agreement with CGYRO results, highlighting the module's reliability, relevance, and utility in NSTX discharges. This alignment between independent simulation methods not only enhances the credibility of MMM's predictive capabilities but also underscores its robustness in describing and predicting plasma behavior in NSTX and related fusion studies.

REFERENCES

[1] RAFIQ, T., KRITZ, A. H., WEILAND, J., PANKIN, A. Y., and LUO, L., Physics of Plasmas **20** (2013) 032506.

[2] BRESLAU, J., GORELENKOVA, M., POLI, F., et al., Transp, [Computer Software] https://doi.org/10.11578/dc.20180627.4, 2018.

[3] RAFIQ, T., WANG, Z., MOROSOHK, S., et al., Plasma **6** (2023) 435.

[4] WEILAND, J., *Stability and Transport in Magnetic Confinement Systems*, Springer, New York, Heidelberg, 2012.

[5] RAFIQ, T., WILSON, C., LUO, L., et al., Physics of Plasmas **29** (2022) 092503.

[6] RAFIQ, T., WEILAND, J., KRITZ, A. H., LUO, L., and PANKIN, A. Y., Physics of Plasmas **23** (2016) 062507.

[7] RAFIQ, T., BATEMAN, G., KRITZ, A. H., and PANKIN, A. Y., Physics of Plasmas **17** (2010) 082511.

[8] CLAUSER, C. F., GUTTENFELDER, W., RAFIQ, T., and SCHUSTER, E., Physics of Plasmas **29** (2022) 102303.

[9] CLAUSER, C. F., RAFIQ, T., SCHUSTER, E. WILSON, C., et al., Studies of ETG transport on NSTX plasmas with gyrokinetics and reduced transport models, in *29th IAEA Fusion Energy Conference (FEC 2023) 16-21 October 2023, London, United Kingdom*, number P1-25, 2023.

[10] RAFIQ, T., KAYE, S., GUTTENFELDER, W., et al., Physics of Plasmas **28** (2021) 022504.